BIOCHEMISTRY
including biophysical chemistry & molecular biology

Article

pubs.acs.org/biochemistry

Site-Specific Conformational Alteration Induced by Sialylation of MUC1 Tandem Repeating Glycopeptides at an Epitope Region for the Anti-KL-6 Monoclonal Antibody

Takahiko Matsushita,[†] Naoki Ohyabu,[†] Naoki Fujitani,[†] Kentaro Naruchi,[‡] Hiroki Shimizu,[§] Hiroshi Hinou,[†,‡] and Shin-Ichiro Nishimura*[,†,‡]

[†]Field of Drug Discovery Research, Faculty of Advanced Life Science, Hokkaido University, Sapporo 001-0021, Japan

[‡]Medicinal Chemistry Pharmaceuticals, Company Ltd., N21, W12, Kita-ku, Sapporo 001-0021, Japan

[§]National Institute of Advanced Industrial Science and Technology, Sapporo 062-8517, Japan

ABSTRACT: Protein O-glycosylation is an essential step for controlling structure and biological functions of glycoproteins involving differentiation, cell adhesion, immune response, inflammation, and tumorigenesis and metastasis. This study provides evidence of site-specific structural alteration induced during multiple sialylation at Ser/Thr residues of the tandem repeats in human MUC1 glycoprotein. Systematic nuclear magnetic resonance (NMR) study revealed that sialylation of the MUC1 tandem repeating glycopeptide, Pro-Pro-Ala-His-Gly-Val-Thr-Ser-Ala-Pro-Asp-Thr-Arg-Pro-Ala-Pro-Gly-Ser-Thr-Ala with core 2-type *O*-glycans at five potential glycosylation sites, afforded a specific conformational change at one of the most important cancer-relevant epitopes (Pro-Asp-Thr-Arg). This result indicates that disease-relevant epitope structures of human epithelial cell surface mucins can be altered both by the introduction of an inner GalNAc residue and by the distal sialylation in a peptide sequence-dependent manner. These data demonstrate the feasibility of NMR-based structural characterization of glycopeptides synthesized in a chemical and enzymatic manner in examining the conformational impact of the distal glycosylation at multiple O-glycosylation sites of mucin-like domains.

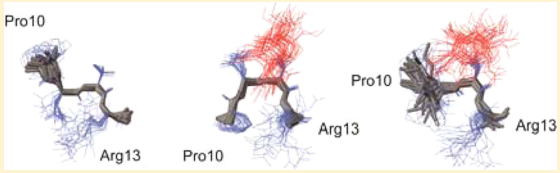

Mucin glycoproteins are widely distributed on epithelial cell surfaces and in organs as a major component of mucosa. They play important functional roles in cell differentiation, proliferation, aging, carcinogenesis, cancer metastasis, and basic immunological systems.[1−4] Multiple O-glycosylation with heterogeneous oligosaccharides at Ser/Thr residues produces densely glycosylated mucin domains, and the mechanism of regulation of this unique structural feature appears to be crucial for controlling biological functions of various mucin glycoproteins. Importantly, the first carbohydrate residue is a conserved GalNAc through α-O-glycosidic linkage to Ser/Thr residues of major mucin glycoproteins, while mature *O*-glycans of normal mammalian mucins have been mostly identified as a mixture of highly complicated oligosaccharide chains.[5−7]

We have focused on the effect of the O-glycosylation processes on the conformations of core proximal peptide moieties of synthetic antifreeze glycoproteins,[8] mucin-type glycopeptides (human MUC1, MUC4, and MUC5AC),[9,10] and EGF-like domain 12 of the mouse Notch-1 receptor.[11] The significance of the first α-O-glycosylation with the GalNAc residue within a clustered locus has been uncovered in the pioneering work of Live et al., who used nuclear magnetic resonance (NMR) to determine the conformation of synthetic glycopeptides, including the N-terminal mucin-like fragment Ser-Thr-Thr-Ala-Val of human T-cell surface glycoprotein CD43.[12] It was suggested that the inner α-GalNAc cluster appears to stabilize the peptide core through the specific interaction between *N*-acetyl methyl groups of GalNAc and methyl groups on the amino acid residues located two residues down the chain. We also revealed a similar mechanism for α-GalNAc residues at the consecutive Thr-Thr moiety in the formation of a highly extended conformation of a tandem repeating peptide, MUC5AC (Pro-Thr-Thr-Val-Gly-Ser-Thr-Thr-Val-Gly), in which the interaction between the *N*-acetyl methyl group of α-GalNAc links to the Thr and methyl group on the Val residue located two residues down the chain.[10] In addition, Corzana et al. reported that the conformational impact of α-O-glycosylation with GalNAc at the Thr residue differs significantly from that at a Ser residue.[13−16] In fact, we demonstrated that hydrogen bonds between the α-GalNAc residue and the threonyl peptide moiety are crucial for the formation of the active conformation of one of the synthetic AFGPs (*sy*AFGP$_3$).[8]

These findings clearly indicate the importance of hydrogen bonds between the proximal peptide moiety involving high-density Thr residue(s) as crucial glycosylation sites and the first α-GalNAc residue in controlling the orientation of glycans with respect to the proximal peptide backbone. Thus, it is clear that conformational impact of glycosylation on the underlying peptide backbone might be one of the most important factors defining biological functions as well as the processes of mucin glycoprotein folding.[11,17−22] Considering that *O*-glycan structures

Received: September 26, 2012
Revised: December 9, 2012
Published: December 21, 2012

   dx.doi.org/10.1021/bi3013142 | *Biochemistry* 2013, 52, 402−414

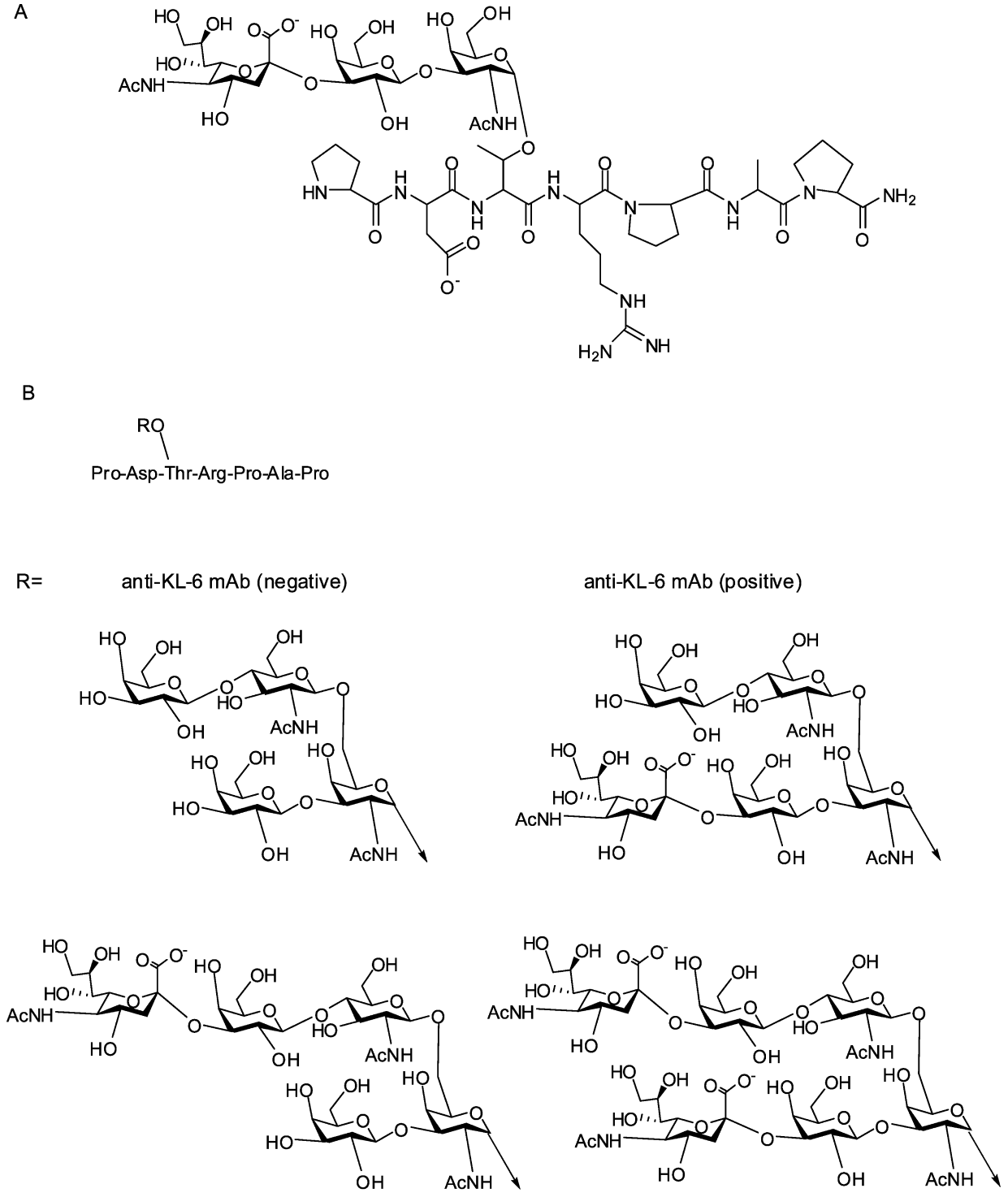

Figure 1. Reactivity of anti-KL-6 mAb with MUC glycopeptides.[9] (A) Minimal epitope structure for anti-KL-6 mAb. (B) Reactivity of anti-KL-6 mAb with MUC1 peptides carrying core 2-type *O*-glycans in this heptapeptide region.

primed at potential glycosylation sites of cell surface mucins are often distinctly altered in the cases of various cancer and immune diseases,[1−7] we hypothesized that glycosylation could affect the antigenic conformation of core proteins, in which particular glycoforms may define or abolish the affinities of monoclonal antibodies (mAbs) with mucins as disease-associated biomarkers.

It is known that α-O-glycosylation at Thr residues by GalNAc forces the peptide backbone into a stable conformation, which minimizes the steric effects by further modifications yielding bulky branched *O*-glycan chains[10,23−25] and serves as the preferred peptide conformation seen in cancer-relevant antigenic structures (epitopes) recognized by some mAbs.[26] In other words, it seems likely that sugar elongation from the inner α-GalNAc residue no longer has any influence on the stable proximal peptide conformation, even though the Golgi biosynthetic pathway might produce a highly complicated *O*-glycan repertoire.

MUC1 is one of the most extensively investigated mucins with great potential as a cancer-related diagnostic and therapeutic target.

dx.doi.org/10.1021/bi3013142 | *Biochemistry* 2013, 52, 402−414

It involves a tandem repeating 20-amino acid sequence, Pro-Pro-Ala-His-Gly-Val-Thr-Ser-Ala-Pro-Asp-Thr-Arg-Pro-Ala-Pro-Gly-Ser-Thr-Ala.[27,28] It is well documented that glycoforms at five potential O-glycosylation sites in this tandem repeat are drastically altered during the differentiation, progression, and metastasis of cancer. However, it was also reported that most mAbs obtained by immunizing a variety of human cancer cells expressing MUC1 exhibited similar broad binding affinities for a few peptide sequences within this tandem repeat.[26,29−33] Antibodies recognizing the Pro-Asp-Thr-Arg motif, a well-characterized MUC1 epitope, are known to have enhanced affinity for this peptide moiety after introduction of α-GalNAc (Tn antigen) at the threonine residue.[34−40] On the other hand, MUC1 glycoproteins of healthy human samples carry highly sialylated *O*-glycans as major glycoforms such as sialyl T, disialyl T, and disialyl core 2-based structures, while average numbers of O-glycosylations at five potential sites seem to be smaller than the number for breast cancer cell line T47D.[41,42]

Recently, we revealed that the minimal epitope for anti-KL-6 mAb, a clinically important probe for diagnosing interstitial pneumonia, lung adenocarcinoma, breast cancer, colorectal adenocarcinoma, and hepatocellular carcinoma,[43−50] is the heptapeptide Pro-Asp-Thr-Arg-Pro-Ala-Pro bearing the sialyl T antigenic trisaccharide (Neu5Acα2,3Galβ1,3GalNAcα1→) of the MUC1 tandem repeat unit.[9] It was demonstrated for the first time that the anti-KL-6 mAb recognizes both heptapeptide and trisaccharide moieties concurrently, in which sialic acid modified at the nonreducing terminus of T antigen (core 1) is an essential component (Figure 1A) while this mAb cannot discriminate between linear core 1 and branched core 2 structures (Figure 1B). Moreover, the binding of anti-KL-6 mAb with this minimal glycopeptide epitope was found to be disturbed by multiple glycosylations with mature core 2-type hexasaccharides at four other potential O-glycosylation sites. Consequently, there was speculation that highly bulky glycan chains, including terminal sialic acids at other glycosylation sites near the epitope, might become a steric hindrance for the specific interaction between anti-KL-6 mAb and this epitope region.[9] Given the fact that normal human cells also express sialyl T and disialyl core 2 structures as major class glycoforms of MUC1,[41,51] our results seem to make a general understanding of functional roles of distal sialylation in mucin antigenicity difficult.

Because a number of anti-MUC1 mAbs require the Pro-Asp-Thr-Arg moiety bearing an inner α-GalNAc residue (Tn antigen) as a minimal epitope,[26,29−40] it is important to uncover the conformational impact of the distal sialylation at this common sequence, as compared with that at other glycosylation sites. We hypothesized that the effect of distal sialylation on this specific peptide sequence may differ from those of four other potential O-glycosylation sites in the MUC1 tandem repeat because maturation of *O*-glycans at this area often appears to lead to the loss of the antigenic nature.

It was clear that the distal sialylation of the T antigen in the MUC1 (KL-6) heptapeptide is essential for the minimal epitope of anti-KL-6 mAb.[9] However, it is noteworthy that T47D, a human breast carcinoma cell line, expresses endogenous MUC1 bearing core 1-based sialyl T antigen as one of its major glycoforms (45.9%), while MCF-7 and ZR75-1 produced dominantly core 2-based *O*-glycans (83% in MCF-7 and 75% in ZR75-1).[42] Importantly, there is no systematic approach to investigating the significance of sialic acid residues in the recognition of MUC1 glycopeptides by known anti-MUC1 mAbs, except the anti-KL-6 mAb.[9] Therefore, it is essential to assess the effect of multiple sialylations on the conformation of individual MUC1 epitopes by focusing on both peptide sequence and site-specific glycan structure. In this study, we performed a comprehensive NMR study to gain insight into the significance of distal glycosylation from the first GalNAc residue attached to the proximal peptide backbone, especially modification by a sialic acid residue, in the conformational regulation of multiple O-glycosylated core 2-type MUC1 glycopeptides.

EXPERIMENTAL PROCEDURES

General Methods and Materials. All commercially available solvents and reagents were used without further purification. Recombinant rat α2,3-(*O*)-SiaT was purchased from Calbiochem (Merck Millipore, Darmstadt, Germany). CMP-Neu5Ac was provided by YAMASA Co. Ltd. (Choshi, Chiba, Japan). All solid-phase reactions for the synthesis were performed manually in a polypropylene tube equipped with a filter. Swelling, washing, acetyl capping, and final cleavage procedures in the solid-phase syntheses were conducted at room temperature. The reaction vessel for solid-phase synthesis was placed inside a cavity of a microwave instrument on a Green Motif I microwave synthesis reactor (IDX Corp., Tochigi, Japan), and the contents were stirred with a vortex mixer. A single-mode microwave was irradiated at 2450 MHz using temperature control at 50 °C.[52] The resulting glycopeptidyl resins were cleaved by being treated with a "cleavage cocktail" solution [TFA/H_2O (95/5, v/v)]. Purification of products was performed on a preparative Hitachi high-performance liquid chromatography (HPLC) system, equipped with an L-7150 intelligent pump and an L-7240 UV detector, using a reversed-phase (RP) C18 column [Inertsil ODS-3, Φ10 × 250 mm or Φ20 × 250 mm (GL Sciences Inc.)]. In enzymatic glycosylation, analysis of the products was performed on a reversed-phase Hitachi HPLC system, equipped with an L-7100 intelligent pump and an L-7405 UV detector, using a reversed-phase (RP) C18 column [Inertsil ODS-3, Φ4.6 × 250 mm (GL Sciences Inc.)]. The following conditions were used for analytical reversed-phase HPLC: elution buffer A, H_2O; elution buffer B, CH_3CN containing 0.1% TFA; linear A/B gradient from 0 to 30 min, 98/2 to 90/10 or 98/2 to 85/15; flow rate, 1.0 mL/min; UV monitoring, 220 nm; column temperature, 40 °C.

NMR Spectroscopy. Glycopeptides were dissolved at a final concentration of 3.0−9.0 mM in 300 μL of a 90% H_2O/10% D_2O mixture or 99% D_2O at pH 5.5. The pH was adjusted to 5.5 by addition of NaOH and HCl. All NMR spectra were observed on a Bruker Avance 600 spectometer with a cryo-probe operating at a proton frequency of 600.03 MHz with a sample temperature of 278 K. For the complete assignments and the determination of the structure of the glycopeptides, two-dimensional DQF-COSY, TOCSY with MLEV-17 sequence, and NOESY spectra were recorded in the indirect dimension using States−TPPI phase cycling.[53] Additionally, two-dimensional heteronuclear ^{13}C-edited HSQC and HSQC-TOCSY measurements were also taken in the echo−antiecho mode for sensitivity enhancement. TOCSY experiments were conducted for a spin-lock time of 60 ms, and NOESY spectra were recorded with mixing times of 100, 150, 200, and 400 ms. The suppression of the water signal was performed by presaturation during the relaxation delay (1 s) and by a 3-9-19 WATERGATE pulse sequence with a field gradient.[54,55] TOCSY and NOESY spectra were acquired with 2048 × 512 frequency data points and were zero-filled to yield 2048 × 2048 data matrices. The DQF-COSY spectrum with 16384 × 512 frequency data points was also recorded and zero-filled

dx.doi.org/10.1021/bi3013142 | *Biochemistry* 2013, 52, 402−414

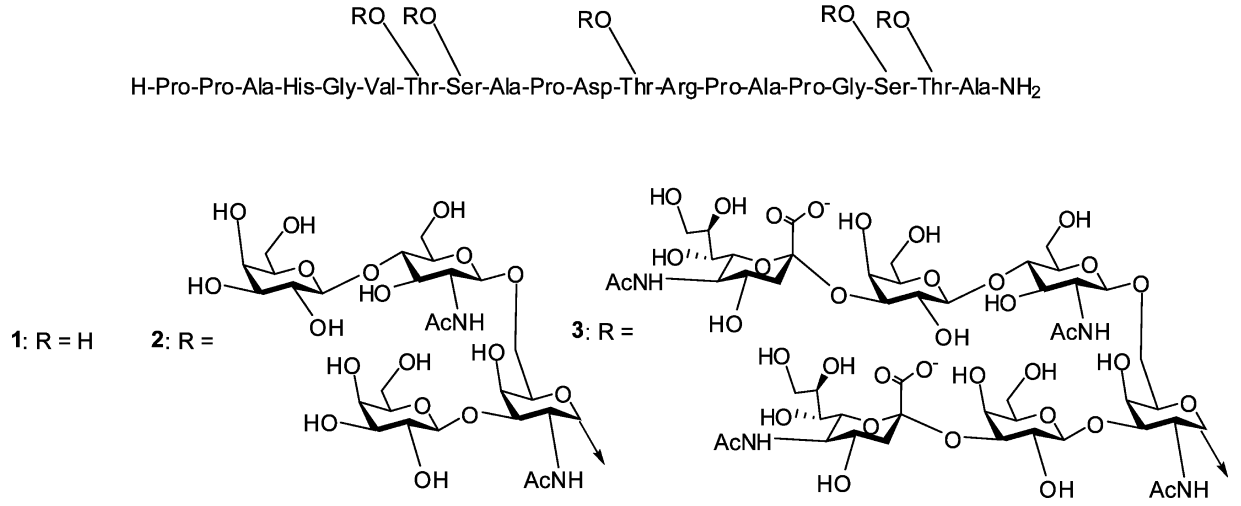

Figure 2. Synthetic MUC1 peptide **1** and glycopeptides **2** and **3** having core 2-type *O*-glycans at five potential glycosylation sites.[63]

to yield a 16384 × 16384 matrix to measure the coupling constants. Sweep widths of 8389.26 Hz were applied. Time domain data in both dimensions were multiplied by a sine bell window function with a 90° phase shift prior to Fourier transformation. All NMR data were processed with NMRPipe[55] and analyzed using Sparky.[56] Sequence-specific resonance assignments were achieved according to the standard methods for small proteins established by Wüthrich and co-workers.[57] Stereospecific assignments for methylene protons were made by analyzing the intensities of intraresidue NOE between amide and β-protons.

Structure Modeling Based on NMR Data. Three-dimensional structures were calculated with CNS 1.1.[58] Distance restraints for calculations were estimated from the cross-peak intensities in NOESY spectra with a mixing time of 200 ms for compounds **2** and **3** and 400 ms for naked MUC1 peptide **1**; the estimated restraints were then classified as strong, medium, weak, and very weak and assigned upper limits of 2.6, 3.5, 5.0, and 6.0 Å, respectively. For NOEs found only in the NOESY spectra with a mixing time of 200 ms, the upper bound was set to 6.0 Å. The restraints of dihedral angle Φ were based on $^3J_{HN\alpha}$ coupling constants measured via high-resolution DQF-COSY. When $^3J_{HN\alpha}$ was more than 8.0 Hz, dihedral angle Φ was constricted to $-120 \pm 30°$ and $-60 \pm 30°$. All analyses of root-mean-square deviation (rmsd) values as well as secondary and tertiary structures were performed with PROCHECK[59] and MOLMOL.[60]

RESULTS AND DISCUSSION

NOEs and Coupling Constants. It was demonstrated that anti-KL-6 mAb shows a high affinity with the MUC1 peptide bearing core 2-type glycans involving the minimal epitope structure such as a disialylated core 2-type hexasaccharide. Therefore, as indicated in Figure 1, we considered that MUC1 analogues **1**−**3** might become suitable models for gaining insight into the conformational impact of distal sialylation on the individual O-glycosylation sites (Figure 2). Glycopeptides **2** and **3** were synthesized efficiently by the chemical and enzymatic strategy[61−69] using a versatile core 2-sugar amino acid building block, Fmoc-Thr/Ser[$Ac_4Gal\beta1,3(Ac_4GlcNAc\beta1,6)$-GalNAc$\alpha$1→]-OH.[63,68,69]

The 600 MHz NMR spectra were recorded at 278 K and pH 5.5 using the previously reported condition.[8,9] Generally, it is well documented that residues consisting of a β-sheet represent a $^3J_{\alpha N}$ value of >8.0 Hz and an α-helix produces a $^3J_{\alpha N}$ value of <6.0 Hz.[70,71] In 20 residues of peptide sequences in the naked MUC1 peptide and glycopeptides **2** and **3**, $^3J_{\alpha N}$ values of >8.0 Hz were identified for five residues (Val6, Thr7, Ser8, Thr12, and Thr19) in the naked peptide and six residues (Val6, Thr7, Ser8, Thr12, Arg13, and Thr19) in **2** and **3** (Figure 3A). These residues suggest the presence of interconverting turn structures and/or an extended structure.[72] Differences in the $^3J_{\alpha N}$ coupling constants of the naked peptide and two glycopeptides also support the local structural alternations caused by the attachment of a core 2-based *O*-glycan involving GalNAcα linking to Thr residues. Indeed, $^3J_{\alpha N}$ values of Thr7, Thr12, and Thr19 increased significantly by 0.5−1 Hz after multiple glycosylations, suggesting that glycosylation involving the GalNAcα1→Thr moiety induces a more extended peptide backbone conformation than those at Ser residues.

A significant number of NOE signals between the peptide core (NH protons of all Ser/Thr residues) and the inner GalNAc residues (NH protons of *N*-acetyl groups) were detected in NOESY spectra of compounds **2** and **3** (Figure 3B). In addition, NH protons of all Thr residues exhibited the characteristic NOE connectivities with methyl protons of the *N*-acetyl groups of the GalNAc moieties.[8,10,12,71] It was demonstrated that these NH protons of the *N*-acetyl groups of GalNAc attached at Thr7, Ser8, Thr12, and Thr19, which corresponded to the residues with a $^3J_{\alpha N}$ value of >8.0 Hz (Figure 3A), have significant NOE connectivities with NH protons of the neighboring amino acid residue, notably GalNAc7-S8, GalNAc7-A9, GalNAc8-A9, GalNAc12-R13, and GalNAc19-A20 (Figure 3B).

The presence of these peptide−sugar NOE signals and the association of GalNAc-attached residues with higher coupling constants suggest that the *N*-acetyl groups of the GalNAc moieties of core 2-based *O*-glycans might be very sensitive to an environmental alteration of the neighboring amino acids during distal glycosylation. As anticipated, the overlay of d_{NN} regions of NOESY spectra indicated that these MUC1 peptides exhibit a large number of strong $d_{\alpha N}(i, i + 1)$ connectivities and strong-to-medium sequential $d_{NN}(i, i + 1)$ connectivities in an immunodominant motif, ^{10}Pro-Asp-Thr-Arg^{13} (Figure 4A). By multiple sialylations at five Thr/Ser residues, some medium and weak $d_{NN}(i, i + 1)$ connectivities in ^{5}Gly-Val-Thr-Ser-Ala^9 and ^{17}Gly-Ser-Thr-Ala^{20} and some medium sequential $d_{\beta N}(i, i + 1)$

dx.doi.org/10.1021/bi3013142 | *Biochemistry* 2013, 52, 402−414

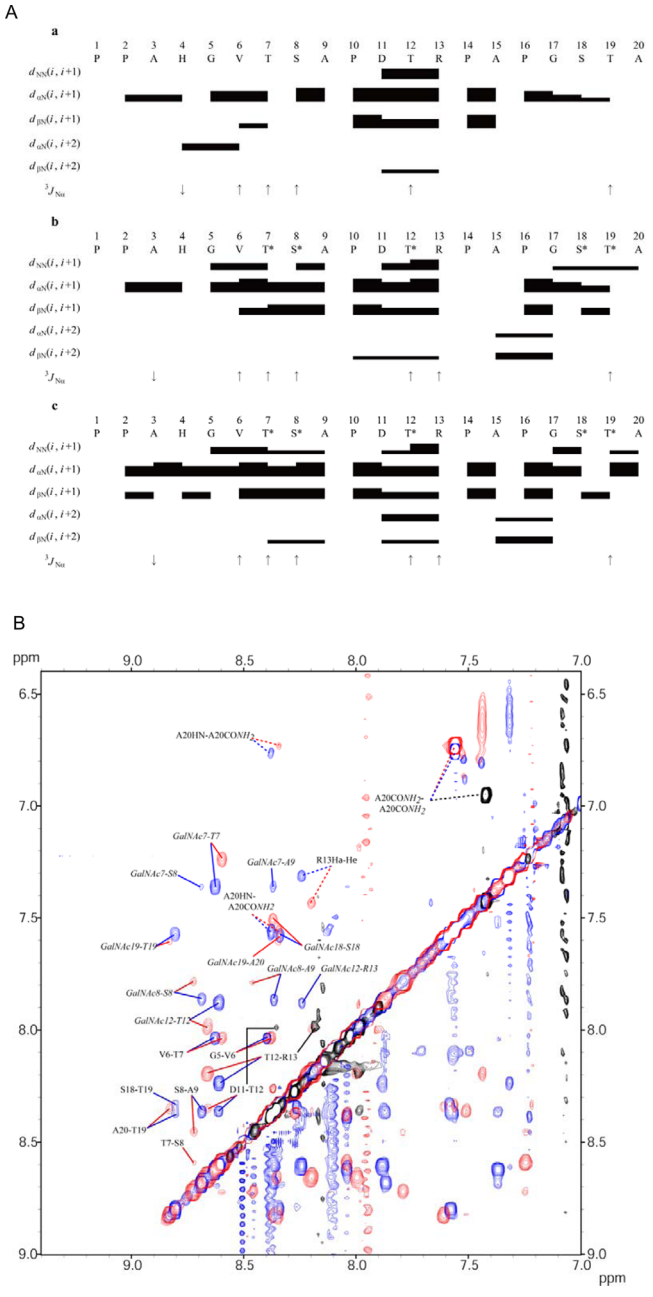

Figure 3. (A) Summary of sequential NOE connectivities, $^{3}J_{N\alpha}$ coupling constants, and angles for MUC1 naked peptide **1** (a), asialo-MUC1 glycopeptide **2** (b), and fully sialylated MUC1 glycopeptide **3** (c). The sequential NOE, d_{NN}, $d_{\alpha N}$, and $d_{\beta N}$ connectivities are represented by the thickness of the respective lines as strong, medium, weak, or very weak. $^{3}J_{N\alpha}$ values of >8 and <6 Hz are indicated by upward arrows and downward arrows, respectively. An asterisk indicates the residue bearing the core 2-based *O*-glycan. (B) Overlay of the d_{NN} regions of the 600 MHz NOESY spectra of **1** (400 ms, black), **2** (200 ms, blue), and **3** (200 ms, red). Both sequential amide−amide cross-peaks in peptide sequences (normal) and cross-peaks between the amide proton of the *N*-acetyl group of the GalNAc moiety and the amide proton of the backbone peptide (italic) are denoted by solid lines. Intraresidue cross-peaks are denoted by dashed lines. GalNAc*X* (*X* = 7, 8, 12, 18, and 19) represents the position of the GalNAc residue attached to the ^{1}PPAHGVTSAPDTRPAPGSTA peptide sequence.

connectivity in ^{7}Thr-Ser-Ala^{9} alternatively were also observed. In the ^{15}Ala-Pro-Gly-Ser-Thr-Ala^{20} region, NOE signals corresponding to $d_{\alpha N}(i, i + 2)$ and $d_{\beta N}(i, i + 2)$ connectivities between Ala15 and Gly17 were newly detected. More importantly, compound **3** showed a medium $d_{\alpha N}(i, i + 2)$ cross-peak between Asp11 and Arg13 and a weak $d_{\beta N}(i, i + 2)$ cross-peak between Thr7 and Ala9, evidence of the structural transition caused by disialylation in this region.

Distal Glycosylation Induces Site-Specific Structural Alteration of the MUC1 Glycopeptide in the PDTR Region. To assess the three-dimensional solution structure of MUC1 (glyco)peptides, we performed structural calculations using CNS[58] with the distance and the dihedral restraints obtained from the NMR experiments. The statistical analyses of NMR restraints and a summary of structural statistics are listed in Table 2. Two hundred-structure ensembles were calculated, and a family of 30 accepted three-dimensional structures were selected with the lowest potential energies. The average dihedral angles and the angle bar plots of ϕ and ψ of these 30 accepted structures are summarized in Table 1 and Figure 4A, respectively. Thus, we compared structural alteration focusing on the three immunodominant motifs, ^{5}Gly-Val-Thr-Ser-Ala^{9} (GVTSA), ^{10}Pro-Asp-Thr-Arg^{13} (PDTR), and ^{17}Gly-Ser-Thr-Ala^{20} (GSTA), during the distal glycosylation from naked MUC1 peptide **1** into core 2-based **2** and fully sialylated glycopeptide **3**.

In the GVTSA segment of the obtained structures of naked MUC1 peptide **1** and glycopeptides **2** and **3**, the pairwise rmsd for the backbone heavy atoms of Val6-Thr7-Ser8 exhibited a descendent tendency (1.80 ± 0.31, 1.19 ± 0.44, and 0.71 ± 0.25 Å, respectively) (Table 2). However, that of Val6-Thr7-Ser8 bearing both GalNAc7 and GalNAc8 in **3** (2.64 ± 0.66 Å) was much larger than that observed in **2** (1.90 ± 0.54 Å), suggesting that core 2-based glycosylation induced a more stabilized and rigid conformation in the GVTSA region of the peptide backbone while sialylation might disturb this conformation.

Differences in the ψ angles of Thr7 and Ser8 among naked MUC1 peptide **1**, **2**, and **3** demonstrated this stabilization effect by glycosylation on the extended peptide backbone structure, while ϕ angles were quite similar to each other (Figure 4A and Table 1). The clusters of ψ angles in Thr7 and Ser8 of glycopeptide **2** appeared to shift into a single, more converged cluster in disialylated **3**. Similar drastic changes in dihedral angles were also observed in the adjacent Val6 residue. The ϕ angle bar plots of Val6 showed good convergence in all compounds, whereas the ψ angle bar plots showed stepwise shifting from dispersed to converged plots among naked MUC1 peptide **1** (35.6 ± 78.3°), **2** (131.2 ± 28.8°), and **3** (166.0 ± 9.5°) in Figure 4A. Furthermore, the χ^{1} angle of Thr7 revealed a significant change caused by glycosylation. The χ^{1} angle of unglycosylated Thr7 (−48.4 ± 82.0°) was considerably different from that of both Thr7 carrying core 2 tetrasaccharide in **2** (45.9 ± 12.9°) and Thr7 carrying disialylated core 2 hexasaccharide in **3** (47.9 ± 7.5°). Considering that the χ^{1} angle is directly related to the particular carbohydrate arrangement, core 2-based O-glycosylation at this Thr7 residue could contribute to the regulation of the glycan orientation.

In addition, the difference in the pairwise rmsd of **3** between Val6-Thr7-Ser8 involving GalNAc7 and GalNAc8 suggested that the disialylated core 2 *O*-glycan introduced at Ser8 appears to be more flexible than that at Thr7 (Table 1 and Figure 4A). Further structural characterizations of the Pro10-Asp11-Thr12-Arg13 (PDTR), Arg13-Pro14-Ala15-Pro16 (RPAP), and Gly17-Ser18-Thr19-Ala20 (GSTA) regions were conducted in

dx.doi.org/10.1021/bi3013142 | *Biochemistry* 2013, 52, 402−414

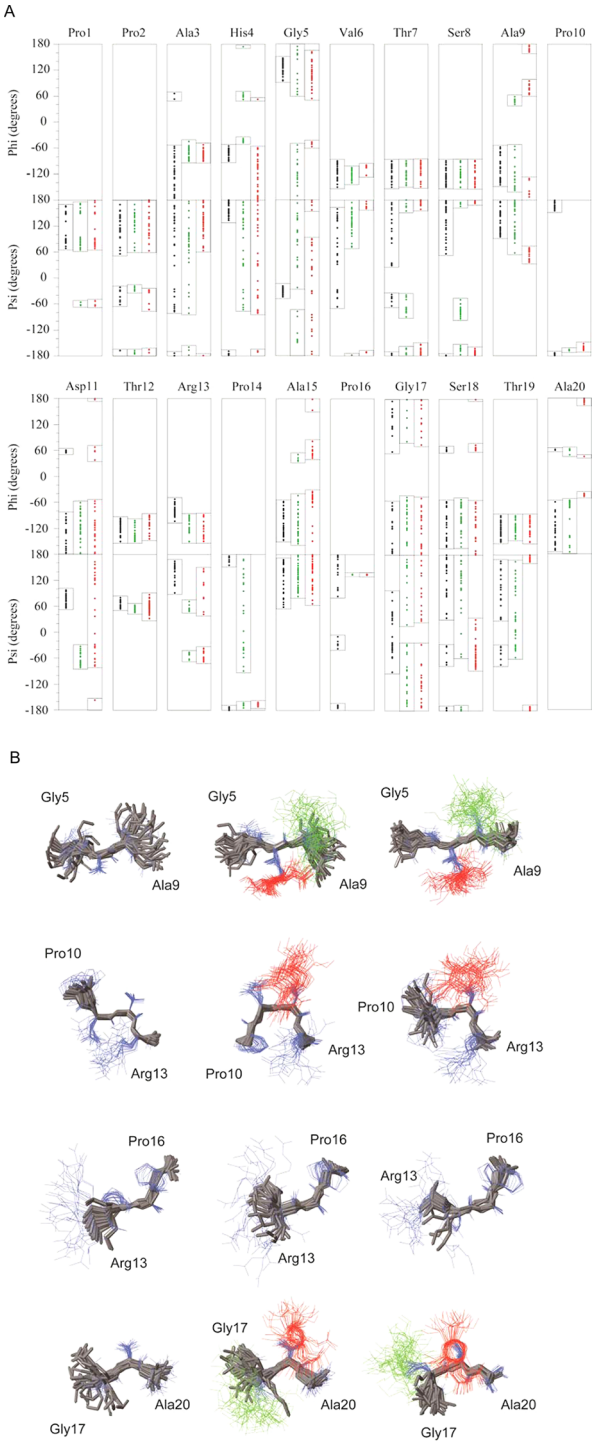

Figure 4. Conformational impact of multiple O-glycosylations of the MUC1 tandem repeat. (A) Angle bar plots of the 30 obtained structures of MUC1 naked peptide **1** (black dots) and glycopeptides **2** (green dots) and **3** (red dots). For all residues except prolines, ϕ and ψ angles are given, and for prolines, ψ angles are given. (B) The 30 best calculated structures from NMR data of MUC1 naked peptide **1** (left) and glycopeptides **2** (middle) and **3** (right). The ^{5}GVTSA^{9}, ^{10}PDTR^{13}, ^{13}RPAP^{16}, and ^{17}GSTA^{20} regions were individually superimposed on the backbone atoms of ^{6}VTS^{8}, ^{11}DTR^{13}, ^{14}PAP^{16}, and ^{18}STA^{20}, respectively. The peptide and glycopeptide structures represent all heavy atoms, including side chains and GalNAc moieties. The main chain of the peptide backbone is colored gray neon; the side chain is shown as a blue line, the GalNAc moiety attached at Thr residue as a red line, and the GalNAc moiety attached at Ser as a green line.

a similar manner. Strikingly, the results clearly show the evidence of the site-specific conformational alteration during multiple O-glycosylations of the MUC1 tandem repeating peptide.

In the PDTR segment, the pairwise rmsd values for the backbone heavy atoms of both Asp11-Thr12-Arg13 and Asp11-Thr12-Arg13 involving GalNAc12 were elevated distinctly during stepwise introduction of the core 2 tetrasaccharide and disialylated core 2 hexasaccharide (Table 2). This may be due to the apparent conformational flexibility between Asp11 and Thr12 as indicated by the fact that the $d_{NN}(i, i + 1)$ connectivity between Asp11 and Thr12 gradually weakened because of O-glycosylation by these glycans (Figure 3). In contrast to the result for the GVTSA region, it was suggested that multiple modifications of the MUC1 peptide by the core 2 tetrasaccharide and disialylated hexasaccharide contribute to the destabilization of the peptide backbone in the PDTR region.

Interestingly, the ϕ and ψ angles of Thr12 were well-ordered in all ensembles (Table 2); this residue did not exhibit higher ψ angles (~60°), while those of Thr7 in GVTSA were −135.8 ± 59.0° (**2**) and −177.2 ± 10.8° (**3**). On the other hand, Kinarsky et al. reported that the ψ angle of Thr in the PDTR motif of MUC1 21-mer naked (unglycosylated) peptide **1** was altered from ~60° to ~160° by enzymatic introduction of the GalNAc residue.[20] This result indicates that an immunodominant DTR motif had an inherent helical conformation, and the GalNAc attachment for this region induced an extended conformation. Our observation clearly demonstrates that the conformational impact of glycosylation by such bulky core 2-based glycans at this position may be significantly different from that of simple glycosylation with the GalNAc residue. The remarkable alternations of dihedral angles were also observed in the Asp11 and Arg13 residues. As compared with the ψ angles of Asp11 in naked MUC1 peptide **1** (71.2 ± 13.8°) and glycopeptide **2** (−64.1 ± 14.1°), both were well fixed, but there was a significant difference.

Furthermore, the ψ angle bar plots of Asp11 in Figure 4A indicate the drastic dispersion at this residue during the conversion from **2** to **3** (108.7 ± 101.1°). Although the χ^1 angles of Arg13 converged well in all ensembles, they displayed a significant change with glycosylation (−80.1 ± 0.1° for naked MUC1 peptide **1** and −164.4 ± 7.3° for **2**), and no significant changes were observed after the disialylation (174.9 ± 10.3° for **3**). These observations suggest clearly that multiple core 2-based O-glycosylations allow for the alteration of both the conformation of the main chain peptide backbone of Asp11 and the orientation of the side chain of Arg13, whereas further full sialylation provided this region with apparent conformational flexibility.

The RPAP segment may often be discussed as the partial structure involved in the most common epitope sequence, PDTRPAP, while this tetrapeptide sequence has no potential O-glycosylation site.[26] The pairwise rmsd for the backbone heavy atoms of Arg13-Pro14-Ala15-Pro16 exhibited no significant difference among three MUC1 derivatives, namely, 0.87 ± 0.39 Å (naked MUC1 **1**), 1.13 ± 0.38 Å (**2**), and 1.16 ± 0.56 Å (**3**) (Table 2). It is noteworthy that multiple glycosylations at neighboring Thr12 induced characteristic changes in the ψ angles of Pro14 and Pro16. Although the ψ angles of Pro14 in naked MUC1 peptide **1** and fully sialylated **3** converged well (178.5 ± 8.5° and 166.5 ± 1.9°, respectively), those of **2** seemed to be more dispersed (170.4 ± 101.3°). On the other hand, the ψ angles of Pro16 in naked MUC1 peptide **1** were dispersed (158.0 ± 90.4°) while those of **2** and **3** converged well (134.8 ± 0.4° and 134.5 ± 0.6°, respectively). It seems likely that multiple glycosylations of

dx.doi.org/10.1021/bi3013142 | *Biochemistry* 2013, 52, 402−414

Table 1. Summary of Dihedral Angles for MUC1 Glycopeptides

		naked MUC1 (1)	asialo core 2 MUC1 (2)	sialyl core 2 MUC1 (3)
Pro1	ψ	109.2 ± 32.4	120.5 ± 82.2	104.1 ± 92.0
Pro2	ψ	116.3 ± 84.4	128.3 ± 78.6	121.0 ± 93.9
Ala3	ϕ	−122.0 ± 58.3	−74.4 ± 13.3	−76.2 ± 12.0
	ψ	124.8 ± 97.0	94.5 ± 75.1	128.8 ± 34.0
	χ^1	105.4 ± 100.6	34.2 ± 95.2	−32.0 ± 88.7
His4	ϕ	−72.1 ± 10.9	11.5 ± 60.4	−112.5 ± 47.9
	ψ	161.4 ± 22.2	106.6 ± 87.1	110.1 ± 100.5
	χ^1	−83.4 ± 75.5	−114.1 ± 66.1	−135.4 ± 89.3
Gly5	ϕ	129.2 ± 26.3	−174.0 ± 78.5	107.5 ± 64.3
	ψ	−26.5 ± 12.3	118.6 ± 78.1	71.2 ± 103.9
Val6	ϕ	−109.8 ± 18.8	−121.2 ± 10.0	−103.3 ± 6.8
	ψ	35.6 ± 78.3	131.2 ± 28.8	166.0 ± 9.5
	χ^1	153.6 ± 67.1	−172.2 ± 45.4	178.7 ± 34.2
Thr7	ϕ	−113.5 ± 19.5	−112.8 ± 20.1	−106.9 ± 18.2
	ψ	112.5 ± 93.1	−135.8 ± 59.0	−177.2 ± 10.8
	χ^1	−43.4 ± 82.0	45.9 ± 12.9	47.9 ± 7.5
Ser8	ϕ	−124.7 ± 18.4	−109.7 ± 21.5	−110.8 ± 24.0
	ψ	137.5 ± 39.4	−131.5 ± 49.5	−174.8 ± 5.5
	χ^1	−48.7 ± 76.9	−102.2 ± 76.9	−85.4 ± 85.6
Ala9	ϕ	−109.6 ± 28.3	−128.2 ± 106.0	118.3 ± 57.9
	ψ	133.7 ± 23.9	136.8 ± 36.7	58.1 ± 9.2
	χ^1	45.3 ± 90.6	65.4 ± 93.4	167.4 ± 89.6
Pro10	ψ	174.5 ± 10.3	−166.8 ± 0.8	−163.5 ± 3.3
Asp11	ϕ	−151.3 ± 89.1	−119.0 ± 33.3	−132.9 ± 70.8
	ψ	71.2 ± 13.8	−64.1 ± 14.1	108.7 ± 101.1
	χ^1	−158.6 ± 25.7	−141.3 ± 24.6	−147.9 ± 52.9
Thr12	ϕ	−116.8 ± 15.6	−136.5 ± 14.4	−104.6 ± 18.7
	ψ	62.8 ± 8.1	53.2 ± 4.0	57.9 ± 13.2
	χ^1	55.2 ± 79.0	49.1 ± 13.2	52.9 ± 15.1
Arg13	ϕ	−79.0 ± 11.9	−111.4 ± 21.3	−109.5 ± 24.1
	ψ	139.7 ± 19.7	−12.1 ± 52.7	−32.5 ± 89.0
	χ^1	−80.1 ± 0.1	−164.4 ± 7.3	174.9 ± 10.3
Pro14	ψ	178.8 ± 8.5	170.4 ± 101.3	−166.5 ± 1.9
Ala15	ϕ	−108.0 ± 27.3	−97.9 ± 60.5	−23.2 ± 77.1
	ψ	131.6 ± 34.2	130.4 ± 26.2	138.8 ± 34.0
	χ^1	17.0 ± 90.2	−105.1 ± 76.7	124.2 ± 92.4
Pro16	ψ	158.0 ± 90.4	134.8 ± 0.4	134.5 ± 0.6
Gly17	ϕ	−172.7 ± 66.6	−104.3 ± 66.7	−149.0 ± 65.7
	ψ	−11.0 ± 47.3	−137.9 ± 84.0	−162.0 ± 92.3
Ser18	ϕ	−108.4 ± 95.0	−88.7 ± 30.0	−116.7 ± 94.8
	ψ	134.5 ± 85.7	133.5 ± 64.5	−47.0 ± 31.5
	χ^1	−64.3 ± 77.4	−125.5 ± 51.5	−98.6 ± 27.1
Thr19	ϕ	−123.3 ± 19.3	−109.2 ± 17.7	−112.4 ± 23.2
	ψ	58.8 ± 77.3	25.8 ± 67.9	179.0 ± 7.5
	χ^1	37.2 ± 78.1	67.6 ± 14.3	56.8 ± 7.3
Ala20	ϕ	−130.9 ± 75.6	−67.0 ± 80.1	−57.9 ± 71.7
	χ^1	−63.7 ± 89.7	−116.8 ± 93.6	−158.9 ± 91.7

naked MUC1 peptide **1** induced a drastic enhancement in the flexibility of Pro14, in contrast to the decrease in the flexibility of Pro16 that yields a more extended conformation. Consequently, disialylation at Thr12 of glycopeptide **2** resulted in the fairly tight extended backbone conformation for Pro14, as found in naked MUC1 peptide **1**, and maintained the extended conformational propensity for the Pro16 residue as observed in **2**.

In the GSTA segment, the pairwise rmsd's for the backbone heavy atoms of Ser18-Thr19-Ala20 in naked MUC1 peptide **1**, glycopeptide **2**, and glycopeptide **3** were 1.61 ± 0.34, 1.32 ± 0.42, and 0.89 ± 0.45 Å, respectively (Table 2). However, that of Ser18-Thr19-Ala20 bearing both GalNAc18 and GalNAc19 in **2** (1.61 ± 0.47 Å) was much smaller than that in **2** (2.44 ± 0.73 Å), suggesting that both core 2-based multiple glycosylations and further disialylation contribute strongly to the stabilization of the GSTA region's conformation in terms of the peptide backbone.

Characteristic alternations in the dihedral angles of Ser18 and Thr19 were observed, especially in the case of fully sialylated **3**. The ψ angles of Ser18 and Thr19 showed similar dispersions in naked MUC1 **1** and glycopeptide **2**, although the ψ angles of Ser18 in fully sialylated **3** exhibited comparatively small convergence to a helical conformation for Ser18 and drastic convergence to an extended conformation for Thr19. The χ^1

dx.doi.org/10.1021/bi3013142 | *Biochemistry* 2013, 52, 402−414

Table 2. Statistical Analysis of NMR Restraints for MUC1 Glycopeptides

	naked MUC1 (**1**)	asialo core 2 MUC1 (**2**)	sialyl core 2 MUCl (**3**)
no. of distance restraints			
total	108	343	448
intraresidue			
peptide	64	117	113
glycan	–	132	231
sequential ($\|i - j\| = 1$)			
peptide	41	70	82
glycan	–	17	16
medium-range ($2 < \|i - j\| < 4$)			
peptide	3	7	6
glycan	–	0	0
long-range ($\|i - j\| > 5$)			
peptide	0	0	0
glycan	–	0	0
peptide to glycan			
within the same glycosylated residue	–	43	40
glycans on other peptide residues	–	20	18
no. of dihedral restraints			
total	7	151	266
peptide backbone	6	7	7
peptide side chain	1	4	4
glycans	–	140	255
	naked MUC1 (**1**)	asialo core 2 MUC1 (**2**)	sialyl core 2 MUC1 (**3**)
average potential energy (kcal/mol)[a]			
E_{total}	9.49 ± 0.29	67.99 ± 3.00	152.8 ± 10.5
E_{bonds}	0.34 ± 0.03	2.48 ± 0.24	4.91 ± 0.55
E_{angle}	6.13 ± 0.11	31.04 ± 1.33	64.31 ± 4.33
E_{impr}[b]	0.57 ± 0.01	9.43 ± 023	17.80 ± 0.56
E_{VDW}[b]	2.30 ± 0.16	7.96 ± 1.45	28.82 ± 3.87
E_{NOE}[b]	0.15 ± 0.12	3.52 ± 0.84	6.63 ± 1.94
E_{cdih}[b]	0.0023 ± 0.003	0.0029 ± 0.036	0.16 ± 0.18
deviation from idealized geometry			
bond lengths (Å)	0.0011 ± 0.0001	0.0018 ± 0.0001	0.0020 ± 0.0001
bond angles (deg)	0.286 ± 0.0026	0.970 ± 0.016	1.063 ± 0.024
impropers (deg)	0.168 ± 0.0011	0.547 ± 0.006	0.614 ± 0.009
average pairwise rmsd (Å)			
backbone atoms			
Val6−Ser8	0.86 ± 0.31	0.61 ± 0.29	0.31 ± 0.14
Asp11−Arg13	0.26 ± 0.12	0.24 ± 0.10	0.58 ± 0.23
Pro14−Pro16	0.42 ± 0.20	0.62 ± 0.20	0.56 ± 0.28
Ser18−Ala20	0.80 ± 0.25	0.78 ± 0.29	0.47 ± 0.25
heavy atoms			
Val6−Ser8	1.80 ± 0.31	1.19 ± 0.44	0.71 ± 0.25
Asp11−Arg13	1.38 ± 0.33	1.46 ± 0.49	1.76 ± 0.49
Pro14−Pro16	0.87 ± 0.39	1.13 ± 0.38	1.16 ± 0.56
Ser18−Ala20	1.61 ± 0.34	1.32 ± 0.42	0.89 ± 0.45
Val6−Ser8 and GaINAc7		1.23 ± 0.36	1.78 ± 0.75
Val6−Ser8 and GaINAc8		1.73 ± 0.57	2.26 ± 0.76
Val6−Ser8, GaINAc7, and GaINAc8		1.90 ± 0.54	2.64 ± 0.66
Asp11−Arg13 and GaINAc12		1.49 ± 0.47	2.05 ± 0.52
Ser18−Ala20 and GaINAc18		2.08 ± 0.68	1.41 ± 0.41
Ser18−Ala20 and GaINAc19		1.45 ± 0.48	1.02 ± 0.38
Ser18−Ala20, GalNAc18, and GaINAc19		2.44 ± 0.73	1.61 ± 0.47

[a]All energies and rmsd values were calculated using CNS 1.1 and MOLMOL, respectively. [b]E_{impr}, E_{VDW}, E_{NOE}, and E_{cdih} are the improper torsion angle energy, the van der Waals repulsion energy, the square-well NOE potential energy, and the dihedral potential energy, respectively. The force constants for the calculations of E_{VDW}, E_{NOE}, and E_{cdih} were 4.0 kcal mol^{-1} Å^{-4}, 50 kcal mol^{-1} Å^{-1}, and 200 kcal mol^{-1} rad^{-2}, respectively.

angles of Thr19 showed similar alternations observed in the Thr7 residue of the GVTSA region. The χ^1 angle of unglycosylated Thr19 (37.2 ± 78.1°) was considerably different from those of both Thr19 bearing a core 2-based tetrasaccharide in **2** (67.6 ± 14.3°) and Thr19 bearing a disialylated core 2 hexasaccharide in **3** (56.8 ± 7.3°). Thus,

dx.doi.org/10.1021/bi3013142 | *Biochemistry* 2013, 52, 402−414

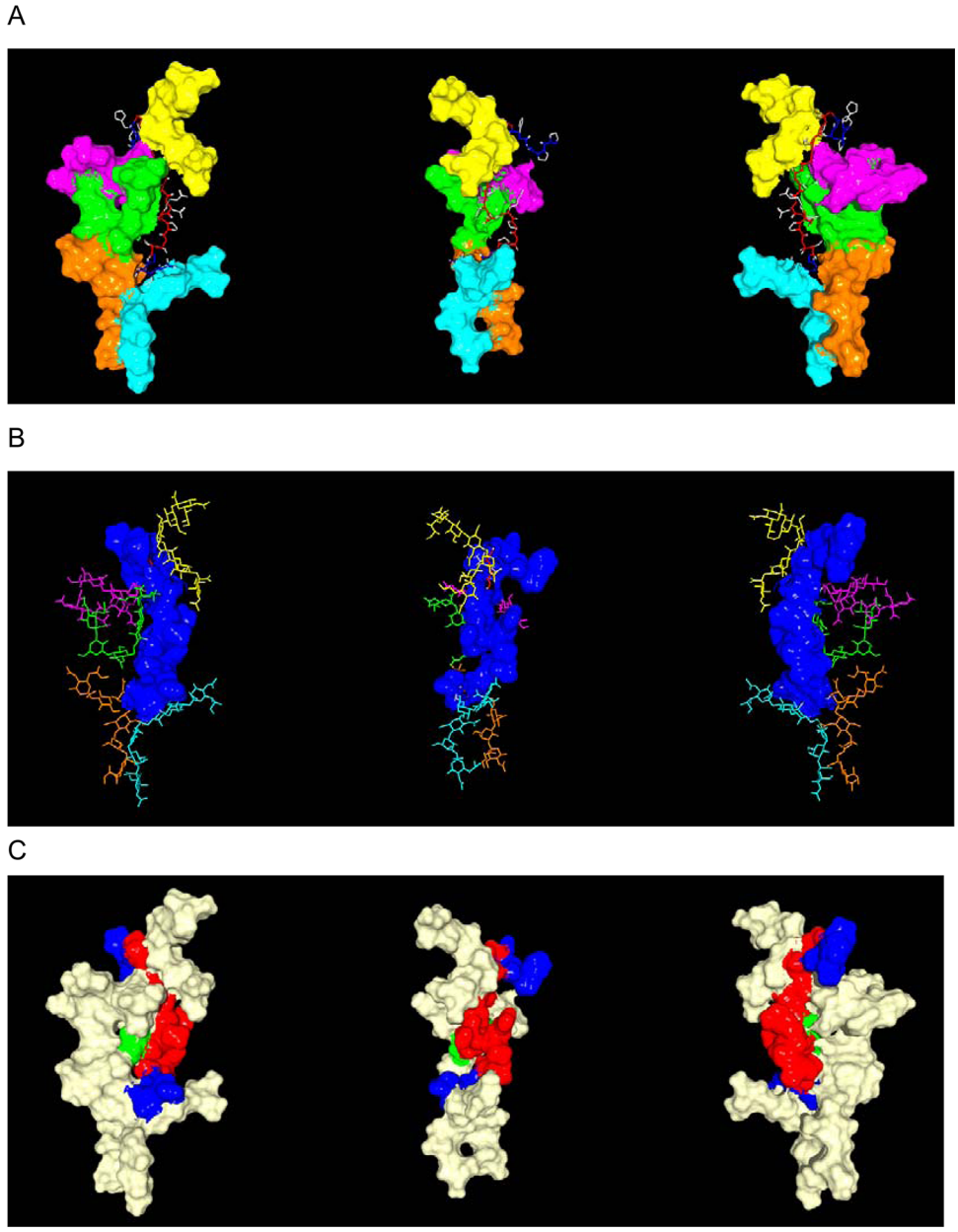

Figure 5. Lowest-energy structure in the 30 calculated models for glycopeptide **3**. The left and right structures are −90° and 90° rotations of the middle structures, respectively. (A) Connolly surfaces of disialyl core 2-based *O*-glycans colored yellow (at Thr7), magenta (at Ser8), green (at Thr12), orange (at Ser18), and aqua (at Thr19). (B) van der Waals surface of the peptide backbone (blue) and five disialyl core 2 hexasaccharide branches indicated by wireframe representations of different colors. (C) van der Waals surface of the backbone peptide with the GalNAc moiety at the PDTR segment (GalNAc12) and the Connolly surfaces of disialyl core 2-based *O*-glycans attached at other glycosylation sites, in which peptide segment ^{5}GVTSAPDTRPAP^{16} is colored red, other segments (^{1}PPAH^{4} and ^{17}GSTA^{20}) are colored blue, and the GalNAc12 moiety is colored green. The Connolly surfaces of other glycan chains are colored white. All of the Connolly surfaces were calculated with a probe radius of 1.4 Å, and these images were generated with Molfeat, version 3.5 (FiatLux).

multiple O-glycosylations could contribute significantly to control the orientation of the Thr19 side chain and the attached *O*-glycans.

Conformational Transition of the PDTR Segment between γ-Turn and β-Turn Structures. The 30 superimposed calculated structures clearly represented the characteristic features of the PDTR and adjacent PAP region, when compared with the three-dimensional structures of GVTSA and GSTA (Figure 4B). The PDTR region of our obtained naked peptide structure ensemble adopted two overlapping inverse γ-turn-like conformations, the first spanning PDT and the second DTR, in which the intraturn hydrogen bond for a γ-turn is formed between the backbone CO (i) and NH (i + 2) groups.[72] The presence of an intraturn hydrogen bond between the backbone CO (i) and NH (i + 2) groups was detected in 6 of 30 and 14 of 30 ensembles in the conformation spanning PDT and DTR, respectively.

Given that the ϕ and ψ angles of the central residue in an inverse γ-turn adopt a $\phi(i+1)$ of −79.0 ± 40° and a $\psi(i+1)$ of 69.0 ± 40°, the dihedral angles of position i + 1 did not satisfy the ideal criteria. However, a clear indication of an inverse γ-turn structure can be made by the $H^{\alpha}(i+1)$–$NH(i+2)$ distance of 2.4 Å, the $NH(i+1)$–$NH(i+2)$ distance of 3.8 Å, and the

dx.doi.org/10.1021/bi3013142 | *Biochemistry* 2013, 52, 402−414

$H^{\alpha}(i)$−NH(i + 2) distance of 4.3 Å. In the lowest-energy ensemble as a representative model, the first conformation spanning PDT revealed only a small difference (<1.0 Å) from the definition of the distance criterion for the ideal inverse γ-turn, an Asp11 $H^{\alpha}(i + 1)$−Thr12 NH(i + 2) distance of 2.4 Å, an Asp11 NH(i + 1)−Thr12 NH(i + 2) distance of 3.0 Å, and a Pro10 $H^{\alpha}(i)$−Thr12 NH(i + 2) distance of 5.3 Å. The second conformation spanning DTR indicated a distance close to that of the ideal inverse γ-turn, a Thr12 $H^{\alpha}(i + 1)$−Arg13 NH(i + 2) distance of 2.4 Å, a Thr12 NH(i + 1)−Arg13 NH(i + 2) distance of 3.5 Å, and an Asp11 $H^{\alpha}(i)$−Arg13 NH(i + 2) distance of 4.3 Å.

On the other hand, the widely accepted definition of a β-turn is that it is comprised of four consecutive residues, where the distance between $C^{\alpha}(i)$ and $C^{\alpha}(i + 3)$ is <7 Å, and that the central residues in the tetrapeptide chain are not in a helical conformation. In the well-ordered PDTR region of our 30 calculated structures of glycopeptide **2**, the lowest-energy model exhibits a distance between Pro10 C_{α} and Arg13 C_{α} of 5.9 Å, fulfilling the distance criterion of a β-turn. This model indicates a distance between Pro10 CO(i) and Arg13 NH(i + 3) of 4.6 Å, suggesting that PDTR has no intraturn hydrogen bond between the backbone CO(i) group and the backbone NH(i + 3) group, which describes an "open turn" as reported by Lewis et al.[73] The dihedral angles of positions i + 1 and i + 2 are not suited for the classification of an ideal β-turn [Asp11 $\phi(i + 1) = -90°$, Asp11 $\psi(i + 1) = -67°$, Thr12 $\phi(i + 2) = -135°$, and Thr12 $\psi(i + 2) = 52°$]. However, the definitions for the distinct type I and type II β-turns are that the distances between $H^{\alpha}(i + 1)$ and NH(i + 2) are 3.6 and 3.3 Å, respectively.[74] The lowest-energy model of **2** predicts a distance of 4.1 Å, indicating that the PDTR region adopts a type I β-turn-like structure spanning PDTR.

Interestingly, the calculated structures of the PDTR regions in fully disialylated **3** seem to be flexibly shifting between the two conformations described above adopted in the same regions in naked peptide **1** (an inverse γ-turn) and in **2** (type I β-turn). Indeed, the PDTR regions of the 30 low-energy structures of **3** were comprised of two clusters that involve 16 and 14 conformers, which were closely similar to naked peptide **1** and to **2**, respectively. As is considered with the PDTR region, the NMR structure model of **3**, therefore, implies that disialylation induces a flexibly shifting set of conformers between an inverse γ-turn-like conformation and a type I β-turn-like conformation. In other words, the distal disialylation of the core 2 tetrasaccharide at Thr12 in glycopeptide **2** might perturb this well-converged type I β-turn-like structure to afford conformational shifting into a more clearly defined extended conformation observed in the ^{5}GVTSA^{9} or ^{17}GSTA^{20} region (Figure 4B).

As shown in Figure 5, a representative model given by the lowest-energy structure of 30 calculated ensembles of glycopeptide **3** appeared to be well reflected in the structural features as described above. Although the importance of this GalNAcα1→Thr motif in the regulation of the conformation of local peptide segments is evident as indicated in Figure 4B, it seems likely that the inner GalNAc moieties linking to the Thr residues exhibit restricted directionalities depending on the fixed side chain orientations.

These limited orientations of the inner GalNAc moieties may contribute to the flexibility and localization of further bulky *O*-glycan structures forming with Neu5Acα2,3Gal and Neu5Acα2,3Galβ1,3GlcNAc chains via β1→3 and β1→6 linkages to GalNAc residues, respectively. This is because both the O3 and O6 involving these linkages are constructed on the same GalNAc framework as well as *N*-acetyl group. In fact, our structural model of compound **3** indicates that the distinct spatial allocations of five individual core 2-based *O*-glycans depend significantly on underlying peptide backbone structures (Figure 5A,B).

In this model, it seemed that the *O*-glycans linking to Ser8, Thr12, and Ser18 localize on the same side of the peptide backbone as they do when forming a consecutive Connolly surface,[75] while those at Thr7 and Thr19 orient toward the opposite side. More importantly, it was discovered that the van der Waals surface of heptapeptide ^{10}PDTRPAP^{16}, a common epitope sequence recognized by various mAbs and represented here in red, remains mostly exposed at Thr12 even after glycosylation compared with other epitope regions such as ^{5}GVTSA^{9} and ^{17}GSTA^{20}. Interestingly, the van der Waals surface of the GalNAc moiety attached at Thr12 (GalNAc12) seems to be shielded considerably by the peptide backbone and other *O*-glycans (Figure 5C). These conformational alterations observed specifically in this region should influence significantly the binding specificity of anti-MUC1 mAbs with an essential sialylated glycopeptide epitope as discovered in the case of anti-KL-6 mAb.[9] Further investigation of the conformational impact of distal sialylation on the antigenicity of various mucin domains is under way by means of a glycopeptide microarray assay as well as NMR studies.

CONCLUSION

Synthetic glycopeptides constructed by a standard protocol based on a chemical and enzymatic strategy are facilitated greatly by structural and functional insight into significance of multiple O-glycosylations in mucin glycoproteins. In this study, we reveal that the conformational impact of distal sialylation is strongly dependent on the peptide core sequence in the tandem repeating domain of MUC1. It was demonstrated that multiple O-glycosylations of the MUC1 tandem repeating peptide give rise to the site-specific conformational impact at the ^{10}PDTRPAP^{16} sequence, known as the most important cancer-relevant epitope region. We discovered that the attachment of a core 2-based tetrasaccharide at Thr12 induces drastic conformational alteration at the PDTR region from a γ-turn-like into β-turn-like structure, accompanied by changes in flexibility in neighboring Pro14 and Pro16 residues. Strikingly, further sialylation induced an interconversion between a β-turn-like and γ-turn-like structure, suggesting that distal sugar modification in this region may greatly influence the essential epitope structure observed in anti-KL-6 mAb.[9]

In contrast, the glycosylation at the other Thr residues contributed only to the stabilization of an extended and rigid conformation of the ^{5}GVTSA^{9} or ^{17}GSTA^{20} region.[76] In addition, further sialylation at these sites did not induce a significant conformational alteration of these sequences. Unfortunately, the effect of the modification by core 2-based *O*-glycans both on the binding profiles with anti-MUC1 mAbs and on the proximal backbone peptide conformation is poorly understood when compared to those of Tn/T antigens as well as sialyl Tn/T motifs.[29−40,71] However, many human breast cancer cells preferentially express core 2-based *O*-glycans terminated mostly with sialic acid with an α2,3 linkage (ZR75-1 and MDA-MB231) and fucose with an α1,3 linkage (MCF-7).[41] Therefore, it is likely that examining the conformational impact of core 2-based *O*-glycans synthesized by C2GnTI[77] and the distal modifications of various mucin motifs is of growing importance for the identification of new classes of disease-relevant epitopes and biomarkers. It should be emphasized that the conformational

dx.doi.org/10.1021/bi3013142 | *Biochemistry* 2013, 52, 402−414

impact by distal sialylation of mucin peptides is strongly dependent on the amino acid sequences involved in the proximal Thr residues to be glycosylated.

AUTHOR INFORMATION

Corresponding Author

*Field of Drug Discovery Research, Faculty of Advanced Life Science, Hokkaido University, Sapporo 001-0021, Japan. E-mail: shin@sci.hokudai.ac.jp. Telephone: +81 11 706 9043.

Funding

This work was partly supported by a grant for "The matching program for innovation in future drug discovery and medical care" from the Ministry of Education, Culture, Science, and Technology, Japan.

Notes

The authors declare no competing financial interest.

REFERENCES

(1) Brockhausen, I. (1999) Pathways of *O*-glycan biosynthesis in cancer cells. *Biochim. Biophys. Acta 1473*, 67−95.

(2) Taylor-Papadimitriou, J. (1999) MUC1 and cancer. *Biochim. Biophys. Acta 1455*, 301−313.

(3) Rosen, S. D. (2004) Ligands for L-selectin: Homing, inflammation, and beyond. *Annu. Rev. Immunol. 22*, 129−156.

(4) Rose, M. C., and Voynow, J. A. (2006) Respiratory tract mucin genes and mucin glycoproteins in health and disease. *Physiol. Rev. 86*, 245−278.

(5) Hollingsworth, M. A., and Swanson, B. J. (2004) Mucins in cancer: Protection and control of the cell surface. *Nat. Rev. Cancer 4*, 45−60.

(6) Ludwig, J. A., and Weinstein, J. N. (2005) Biomarkers in cancer staging, prognosis and treatment selection. *Nat. Rev. Cancer 5*, 845−856.

(7) Dube, D. H., and Bertozzi, C. R. (2005) Glycans in cancer and inflammation. Potential for therapeutics and diagnostics. *Nat. Rev. Drug Discovery 4*, 477−488.

(8) Tachibana, Y., Fletcher, G. L., Fujitani, N., Tsuda, S., Monde, K., and Nishimura, S.-I. (2004) Antifreeze glycoproteins: Elucidation of the structural motifs that are essential for antifreeze activity. *Angew. Chem., Int. Ed. 43*, 856−862.

(9) Ohyabu, N., Hinou, H., Matsushita, T., Izumi, R., Shimizu, H., Kawamoto, K., Numata, Y., Togame, H., Takemoto, H., Kondo, H., and Nishimura, S.-I. (2009) An Essential Epitope of Anti-MUC1 Monoclonal Antibody KL-6 Revealed by Focused Glycopeptide Library. *J. Am. Chem. Soc. 131*, 17102−17109.

(10) Hashimoto, R., Fujitani, N., Takegawa, Y., Kurogochi, M., Matsushita, T., Naruchi, K., Ohyabu, N., Hinou, H., Gao, X.-D., Manri, N., Satake, H., Kaneko, A., Sakamoto, T., and Nishimura, S.-I. (2011) An Efficient Approach for the Characterization of Mucin-Type Glycopeptides: The Effect of *O*-Glycosylation on the Conformation of Synthetic Mucin Peptides. *Chem.—Eur. J. 17*, 2393−2404.

(11) Shimizu, K. H., Hosoguchi, K., Liu, Y., Fujitani, N., Ohta, T., Hinou, H., Matsushita, T., Shimizu, H., Feizi, T., and Nishimura, S.-I. (2010) Chemical Synthesis, Folding, and Structural Insights into *O*-Fucosylated Epidermal Growth Factor-like Repeat 12 of Mouse Notch-1 Receptor. *J. Am. Chem. Soc. 132*, 14857−14865.

(12) Coltart, D. M., Royyuru, A. K., Williams, L. J., Glunz, P. W., Sames, D., Kuduk, S. D., Schwarz, J. B., Chen, X.-T., Danishefsky, S. J., and Live, D. H. (2002) Principles of mucin architecture: Structural studies on synthetic glycopeptides bearing clustered mono-, di-, tri-, and hexasaccharide glycodomains. *J. Am. Chem. Soc. 124*, 9833−9844.

(13) Corzana, F., Busto, J. H., Osés, G. J., Asensio, J. L., Barbero, J. J., Peregrina, J. M., and Avenoza, A. (2006) New insights into α-GalNAc-Ser motif: Influence of hydrogen bonding versus solvent interactions on the preferred conformation. *J. Am. Chem. Soc. 128*, 14640−14684.

(14) Corzana, F., Busto, J., Engelsen, S. B., Barbero, J. J., Asensio, J. L., Peregrina, J. M., and Avenoza, A. (2006) Effect of β-*O*-glucosylation on L-Ser and L-Thr diamides: A bias toward α-helical conformations. *Chem.—Eur. J. 12*, 7864−7871.

(15) Corzana, F., Busto, J. H., Osés, G. J., de Luis, M. G., Asensio, J. L., Barbero, J. J., Peregrina, J. M., and Avenoza, A. (2007) Serine versus threonine glycosylation: The methyl group causes a drastic alteration on the carbohydrate orientation and on the surrounding water shell. *J. Am. Chem. Soc. 129*, 9458−9467.

(16) Corzana, F., Busto, J. H., de Luis, M. G., Barbero, J. J., and Avenoza, A. (2009) The Nature and Sequence of the Amino Acid Aglycone Strongly Modulates the Conformation and Dynamics Effects of Tn Antigen's Clusters. *Chem.—Eur. J. 15*, 3863−3874.

(17) Live, D. H., Williams, L. J., Kuduk, S. D., Schwarz, J. B., Glunz, P. W., Chen, X.-T., Sames, D., Kumar, R. A., and Danishefsky, S. J. (1999) Probing cell-surface architecture through synthesis: An NMR-determined structural motif for tumor-associated mucins. *Proc. Natl. Acad. Sci. U.S.A. 96*, 3489−3493.

(18) Kirnarsky, L., Prakash, O., Vogen, S. M., Nomoto, M., Hollingsworth, M. A., and Sherman, S. (2000) Structural effects of *O*-glycosylation on a 15-residue peptide from the mucin (MUC1) core protein. *Biochemistry 39*, 12076−12082.

(19) Wormald, M. R., Petrescu, A. J., Pao, Y. L., Glithero, A., Elliott, T., and Dwek, R. A. (2002) Conformational studies of oligosaccharides and glycopeptides: Complementarity of NMR, X-ray crystallography, and molecular modelling. *Chem. Rev. 102*, 371−386.

(20) Kinarsky, L., Suryanarayanan, G., Prakash, O., Paulsen, H., Clausen, H., Hanisch, F.-G., Hollingsworth, M. A., and Sherman, S. (2003) Conformational studies on the MUC1 tandem repeat glycopeptides: Implication for the enzymatic *O*-glycosylation of the mucin protein core. *Glycobiology 13*, 929−939.

(21) Jinek, M., Chen, Y.-W., Clausen, H., Cohen, S. M., and Conti, E. (2006) Structural insights into the Notch-modifying glycosyltransferase Fringe. *Nat. Struct. Mol. Biol. 13*, 945−946.

(22) Kuhn, A., and Kunz, H. (2007) Saccharide-induced peptide conformation in glycopeptides of the recognition region of LI-cadherin. *Angew. Chem., Int. Ed. 46*, 454−458.

(23) Ten Hagen, K. G., Fritz, T. A., and Tabak, L. A. (2003) All in the family: The UDP-GalNAc:polypeptide N-acetylgalactosaminyl-transferases. *Glycobiology 13*, 1−16.

(24) Ju, T., Otto, V. I., and Cummings, R. D. (2011) The Tn Antigen-Structural Simplicity and Biological Complexity. *Angew. Chem., Int. Ed. 50*, 1770−1791.

(25) Borgert, A., Heimburg-Molinaro, J., Song, X., Lasanajak, Y., Ju, T., Liu, M., Thompson, P., Ragpathi, G., Barany, U., Smith, D. F., Cummings, R. D., and Live, D. (2012) Deciphering structural elements of mucin glycoprotein recognition. *ACS Chem. Biol. 7*, 1031−1039.

(26) Prince, M. R., Rye, P. D., Petrakou, E., Murray, A., Brady, K., Imai, S., Haga, S., Kiyozuka, Y., Schol, D., Meulenbroek, M. F., Snijdewint, F. G., von Mensdorff-Pouilly, S., Verstraeten, R. A., Kenemans, P., Blockzjil, A., Nilsson, K., Nilsson, O., Reddish, M., Suresh, M. R., Koganty, R. R., Forter, S., Baronic, L., Berg, A., Longenecker, M. B., and Higers, J. (1998) Summary Report on the ISOBM TD-4 Workshop: Analysis of 56 Monoclonal Antibodies against the MUC1Mucin. *Tumor Biol. 19*, 1−20.

(27) Hattrup, C. L., and Gendler, S. J. (2008) Structure and function of the cell surface (tethered) mucins. *Annu. Rev. Physiol. 70*, 431−457.

(28) Tarp, M. A., and Clausen, H. (2009) Mucin-type *O*-glycosylation and its potential use in drug and vaccine development. *Biochim. Biophys. Acta 1780*, 546−563.

(29) Springer, G. F. (1984) T and TN, general carcinoma auto-antigens. *Science 224*, 1198−1206.

(30) Taylor-Papadimitriou, J., and Epenetos, A. A. (1994) Exploiting altered glycosylation patterns in cancer: Progress and challenges in diagnosis and therapy. *Trends Biotechnol. 12*, 227−233.

(31) Lloyd, K. O., Burchell, J., Kudryashov, V., Yin, B. W. T., and Taylor-Papadimitriou, J. (1996) Comparison of *O*-linked carbohydrate chains in MUC-1 mucin from normal breast epithelial cell lines and breast carcinoma cell lines: Demonstration of simpler and fewer glycan chains in tumor cells. *J. Biol. Chem. 271*, 33325−33334.

(32) Brockhausen, I. (1999) Pathways of *O*-glycan biosynthesis in cancer cells. *Biochim. Biophys. Acta 1473*, 67−95.
(33) Burchell, J. M., Mungul, A., and Taylor-Papadimitriou, J. (2001) *O*-linked glycosylation in the mammary gland: Changes that occur during malignancy. *Journal of Mammary Gland Biology and Neoplasia 6*, 355−363.
(34) Hanisch, F.-G., Standie, T., and Bosslet, K. (1995) Monoclonal-antibody BW835 defines a site-specific Thomsen-Friedenreich disaccharide linked to threonine within the VTSA motif of MUC1 tandem repeats. *Cancer Res. 55*, 4036−4040.
(35) Dai, J., Allard, W. J., Davis, G., and Yeung, K. K. (1998) Effect of desialylation on binding, affinity, and specificity of 56 monoclonal antibodies against MUC1 mucin. *Tumor Biol. 19*, 100−110.
(36) Grinstead, J. S., Koganty, R. R., Krantz, M. J., Longencker, B. M., and Campbell, A. P. (2002) Effect of glycosylation on MUC1 humoral immune recognition: NMR studies of MUC1 glycopeptide-antibody interactions. *Biochemistry 41*, 9946−9961.
(37) Takeuchi, H., Kato, K., da-Nagai, K., Hanisch, F. G., Clausen, H., and Irimura, T. (2002) The epitope recognized by the unique anti-MUC1 monoclonal antibody MY.1E12 involves sialyl α2−3galactosyl β1−3N-acetylgalactosaminide linked to a distinct threonine residue in the MUC1 tandem repeat. *J. Immunol. Methods 270*, 199−209.
(38) Grinstead, J. S., Schuman, J. T., and Campbell, A. P. (2003) Epitope mapping of antigenic MUC1 peptides to breast cancer antibody fragment B27.29: A heteronuclear NMR study. *Biochemistry 42*, 14293−14305.
(39) Danielczyk, A., Stahn, R., Faulstich, D., Löffler, A., Märten, A., Karsten, U., and Goletz, S. (2006) PankoMab: A potent new generation anti-tumour MUC1 antibody. *Cancer Immunol. Immunother. 55*, 1337−1347.
(40) Tarp, M. A., Sørensen, A. L., Mandel, U., Paulsen, H., Burchell, G. M., Taylor-Papadimitriou, J., and Clausen, H. (2007) Identification of a novel cancer-specific immunodominant glycopeptide epitope in the MUC1 tandem repeat. *Glycobiology 17*, 197−209.
(41) Müller, S., Goletz, S., Packer, N., Gooley, A., Lawson, A. M., and Hanisch, F.-G. (1997) Localization of *O*-glycosylation sites on glycopeptide fragments from lactation-associated MUC1: All putative sites within the tandem repeat are glycosylation targets *in vivo*. *J. Biol. Chem. 272*, 24780−24793.
(42) Müller, S., and Hanisch, F.-G. (2002) Recombinant MUC1 probe authentically reflects cell-specific *O*-glycosylation profiles of endogenous breast cancer mucin: High density and prevalent core 2-based glycosylation. *J. Biol. Chem. 277*, 26103−26112.
(43) Kohno, N., Akiyama, M., Kyoizumi, S., Hakoda, M., Kobuke, K., and Yamakido, M. (1988) Detection of soluble tumor-associated antigens in sera and effusions using novel monoclonal antibodies, KL-3 and KL-6, against lung adenocarcinoma. *Jpn. J. Clin. Oncol. 18*, 203−216.
(44) Ogawa, Y., Ishikawa, T., Ikeda, K., Nakada, B., Sawada, T., Ogisawa, K., Kato, Y., and Hirasawa, K. (2000) Evaluation of serum KL-6, a mucin-like glycoprotein, as a tumor marker for breast cancer. *Clin. Cancer Res. 6*, 4069−4072.
(45) Hirasawa, Y., Kohno, N., Yokoyama, A., Kondo, K., Hiwada, K., and Miyake, M. (2000) Natural autoantibody to MUC1 is a prognostic indicator for non-small cell lung cancer. *Am. J. Respir. Crit. Care Med. 161*, 589−594.
(46) Kurosaki, M., Izumi, N., Onuki, Y., Nishimura, Y., Ueda, K., Tsuchiya, K., Nakanishi, H., Kitamura, T., Asahina, Y., Uchihara, M., and Miyake, S. (2005) Serum KL-6 as a novel tumor marker for hepatocellular carcinoma in hepatitis C virus infected patients. *Hepatol. Res. 33*, 250−257.
(47) Amal, G., Tanaka, E., Matsumoto, A., Abd-el Wahab, M., Serwah, el-H., Attia, F., Ali, K., Hassouba, H., el-Deeb, A. el-R., Ichijo, T., Umemura, T., Huto, H., Yoshizawa, K., and Kiyosawa, K. (2005) Assessment of KL-6 as a tumor marker in patients with hepatocellular carcinoma. *World J. Gastroenterol. 11*, 6607−6612.
(48) Guo, Q., Tang, W., Inagaki, Y., Midorikawa, Y., Kokudo, N., Sugawara, Y., Nakata, M., Konishi, T., Nagawa, H., and Makuuchi, M. (2006) Clinical significance of subcellular localization of KL-6 mucin in primary colorectal adenocarcinoma and metastatic tissues. *World J. Gastroenterol. 12*, 54−59.
(49) Inata, J., Hattori, N., Yokoyama, A., Ohshiro, S., Doi, M., Ishikawa, N., Hamada, H., and Kohno, N. (2007) Circulating KL-6/MUC1 mucin carrying sialyl Lewis(a) oligosaccharide is an independent prognostic factor in patients with lung adenocarcinoma. *Int. J. Cancer 120*, 2643−2649.
(50) Ishikawa, N., Hattori, N., Yokoyama, A., Tanaka, S., Nishino, R., Yoshikawa, K., Ohshimo, S., Fujitaka, K., Ohnishi, H., Hamada, H., Arihiro, K., and Kohno, N. (2008) Usefulness of monitoring the circulating Krebs von den Lungen-6 levels to predict the clinical outcome of patients with advanced nonsmall cell lung cancer treated with epidermal growth factor receptor tyrosine kinase inhibitors. *Int. J. Cancer 122*, 2612−2620.
(51) Miura, Y., Kato, K., Takegawa, Y., Kurogochi, M., Furukawa, J., Shinohara, Y., Nagahori, N., Amano, M., Hinou, H., and Nishimura, S.-I. (2010) Glycoblotting-Assisted *O*-Glycomics: Ammonium Carbamate Allows for Highly Efficient *O*-Glycan Release from Glycoproteins. *Anal. Chem. 82*, 10021−10029.
(52) Matsushita, T., Hinou, H., Kurogochi, M., Shimizu, H., and Nishimura, S.-I. (2005) Rapid microwave-assisted solid-phase glycopeptide synthesis. *Org. Lett. 7*, 877−880.
(53) Bothner-By, A. A., Stephens, R. L., Lee, J.-M., Warren, C. D., and Jeanloz, R. W. (1984) Structure determination of a tetrasaccharide: Transient nuclear Overhauser effects in the rotating frame. *J. Am. Chem. Soc. 106*, 811−813.
(54) Bax, A., and Davis, D. G. (1985) Practical aspects of two-dimensional transverse NOE spectroscopy. *J. Magn. Reson. 63*, 207−213.
(55) Piotto, M., Saudek, V., and Sklenár, V. (1992) Gradient-tailored excitation for single-quantum NMR-spectroscopy of aqueous-solutions. *J. Biomol. NMR 2*, 661−665.
(56) Delaglio, F., Grzesiek, S., Vuister, G., Zhu, G., Pfeifer, J., and Bax, A. (1995) NMRPIPE: A multidimensional spectral processing system based on UNIX PIPES. *J. Biomol. NMR 6*, 277−293.
(57) Goddard, T. D., and Kneller, D. G. (2008) *SPARKY 3*, University of California, San Francisco.
(58) Brünger, A. T., Adams, P. D., Clore, G. M., DeLano, W. L., Gros, P., Grosse-Kunstleve, R. W., Jiang, J. S., Kuszewski, J., Nilges, M., Pannu, N. S., Read, R. J., Rice, L. M., Simonson, T., and Warren, G. L. (1998) Crystallography & NMR system: A new software suite for macromolecular structure determination. *Acta Crystallogr. D54*, 905−921.
(59) Laskowski, R. A., Rullmann, J. A. C., MacArthur, M. W., Kaptein, R., and Thornton, J. M. (1996) AQUA and PROCHECK-NMR: Programs for checking the quality of protein structures solved by NMR. *J. Biomol. NMR 8*, 477−486.
(60) Koradi, R., Billeter, M., and Wüthrich, K. (1996) MOLMOL: A program for display and analysis of macromolecular structures. *J. Mol. Graphics 14*, 51−55.
(61) Fumoto, M., Hinou, H., Matsushita, T., Kurogochi, M., Ohta, T., Ito, T., Yamada, K., Takimoto, A., Kondo, H., Inazu, T., and Nishimura, S.-I. (2005) Molecular transporter between polymer platforms: Highly efficient chemoenzymatic glycopeptide synthesis by the combined use of solid-phase and water-soluble polymer supports. *Angew. Chem., Int. Ed. 44*, 2534−2537.
(62) Fumoto, M., Hinou, H., Ohta, T., Ito, T., Yamada, K., Takimoto, A., Kondo, H., Shimizu, H., Inazu, T., Nakahara, Y., and Nishimura, S.-I. (2005) Combinatorial synthesis of MUC1 glycopeptides: Polymer blotting facilitates chemical and enzymatic synthesis of highly complicated mucin glycopeptides. *J. Am. Chem. Soc. 127*, 11804−11818.
(63) Matsushita, T., Hinou, H., Fumoto, M., Kurogochi, M., Fujitani, N., Shimizu, H., and Nishimura, S.-I. (2006) Construction of highly glycosylated mucin-type glycopeptides based on microwave-assisted solid-phase syntheses and enzymatic modifications. *J. Org. Chem. 71*, 3051−3063.
(64) Naruchi, K., Hamamoto, T., Kurogochi, M., Hinou, H., Shimizu, H., Matsushita, T., Fujitani, N., Kondo, H., and Nishimura, S.-I. (2006)

Construction and structural characterization of versatile lactosaminoglycan-related compound library for the synthesis of complex glycopeptides and glycosphingolipids. *J. Org. Chem. 71*, 9609−9621.
(65) Matsushita, T., Sadamoto, R., Ohyabu, N., Nakata, H., Fumoto, H., Fujitani, N., Takegawa, Y., Sakamoto, T., Kurogochi, M., Hinou, H., Shimizu, H., Ito, T., Naruchi, K., Togame, H., Takemoto, H., Kondo, H., and Nishimura, S.-I. (2009) Functional Neoglycopeptides: Synthesis and Characterization of a New Class of MUC1 Glycoprotein Models Having Core 2-Based *O*-Glycan and Complex-Type N-Glycan Chains. *Biochemistry 48*, 11117−11133.
(66) Matsushita, T., Nagashima, I., Fumoto, M., Ohta, T., Yamada, K., Shimizu, H., Hinou, H., Naruchi, K., Ito, T., Kondo, H., and Nishimura, S.-I. (2010) Artificial Golgi Apparatus: Globular Protein-like Dendrimer Facilitates Fully Automated Enzymatic Glycan Synthesis. *J. Am. Chem. Soc. 132*, 16651−16656.
(67) Naruchi, K., and Nishimura, S.-I. (2011) Membrane-Bound Stable Glycosyltransferases: Highly Oriented Protein Immobilization by a C-Terminal Cationic Amphipathic Peptide. *Angew. Chem., Int. Ed. 80*, 1328−1331.
(68) Meinjohannes, E., Meldal, M., Schleyer, A., Paulsen, H., and Bock, K. (1996) Efficient syntheses of core 1, core 2, core 3 and core 4 building blocks for SPS of mucin *O*-glycopeptides based on the N-Dts-method. *J. Chem. Soc., Perkin Trans. 1*, 985−993.
(69) Mathieux, N., Paulsen, H., Meldal, M., and Bock, B. (1997) Synthesis of glycopeptide sequences of repeating units of the mucins MUC 2 and MUC 3 containing oligosaccharide side-chains with core 1, core 2, core 3, core 4 and core 6 structure. *J. Chem. Soc., Perkin Trans. 1*, 2359−2368.
(70) Wüthrich, K. (1986) *NMR of Proteins and Nucleic Acids*, John Wiley and Sons, New York.
(71) Grinstead, J. S., Koganty, R. R., Krantz, M. J., Longencker, B. M., and Campbell, A. P. (2002) Effect of glycosylation on MUC1 humoral immune recognition: NMR studies of MUC1 glycopeptide-antibody interactions. *Biochemistry 41*, 9946−9961.
(72) Milner-White, E. J., Ross, B. M., Ismail, R., Belhadj-Mostefa, K., and Poet, R. (1988) One type of γ-turn, rather than the other gives rise to chain-reversal in proteins. *J. Mol. Biol. 204*, 777−782.
(73) Lewis, P. N., Momany, F. A., and Scheraga, H. A. (1973) Chain reversals in proteins. *Biochim. Biophys. Acta 303*, 211−229.
(74) Wüthrich, K., Billeter, M., and Braun, W. (1984) Polypeptide secondary structure determination by nuclear magnetic-resonance observation of short proton proton distances. *J. Mol. Biol. 180*, 715−740.
(75) Connolly, M. L. (1983) Analytical molecular-surface calculation. *J. Appl. Crystallogr. 16*, 548−558.
(76) Dziadek, S., Griesinger, C., Kunz, H., and Reinscheid, U. M. (2006) Synthesis and structural model of an α(2,6)-sialyl-T glycosylated MUC1 eicosapeptide under physiological conditions. *Chem.—Eur. J. 12*, 4981−4993.
(77) Tsuboi, S., Sutoh, M., Hatakeyama, S., Hiraoka, N., Habuchi, T., Horikawa, Y., Hashimoto, Y., Yoneyama, T., Mori, K., Koie, T., Nakamura, T., Saitoh, H., Yamaya, K., Funyu, T., Fukuda, M., and Ohyama, C. (2011) A novel strategy for evasion of NK cell immunity by tumours expressing core 2 *O*-glycans. *EMBO J. 30*, 3173−3185.